Enhanced bioaffinity sensing using surface plasmons, surface enzyme reactions, nanoparticles and diffraction gratings†‡

Hye Jin Lee,*[a] Alastair W. Wark[b] and Robert M. Corn[c]

Received 5th December 2007, Accepted 29th February 2008
First published as an Advance Article on the web 13th March 2008
DOI: 10.1039/b718713k

This paper introduces a novel approach to surface bioaffinity sensing based on the adsorption of nanoparticles onto a gold diffraction grating that supports the excitation of planar surface plasmons. A surface enzymatic amplification reaction is also incorporated into the detection scheme to enhance the sensitivity and utility of the nanoparticle-enhanced diffraction grating (NEDG) sensors. As a demonstration, the detection of microRNA is described where a combination of a surface polymerase reaction and DNA-modified nanoparticles is used to detect the bioaffinity adsorption of the target onto the probe-functionalized gold grating surface. The enzymatically-amplified NEDG sensors possess a great potential for a wide range of applications including the detection of biosecurity agents, DNA and RNA viruses, biomarkers, and proteins.

1. Introduction

Surface bioaffinity sensors have become invaluable and extremely versatile tools for the rapid, multiplexed detection of biomolecular and chemical species. Through careful surface immobilization of an appropriate capture probe biomolecule, it is possible to create detection platforms that are highly selective towards a specific target present in complex testing environments. To monitor surface bioaffinity interactions a variety of surface-sensitive spectroscopic techniques have been developed over the last decade or so. In particular, surface plasmon resonance (SPR) has emerged as an excellent alternative to traditional fluorescence-based measurements as it offers label-free detection without the need for modification of the target molecules prior to analysis. For example, the technique of SPR imaging (SPRI), where multiple probes are arrayed on a single planar gold thin film, has been successfully applied to measure the bioaffinity adsorption of DNA, RNA, antibodies, proteins and biomarkers.[1–7]

In addition to enabling advances in the biodiagnostic and molecular biology research fields, SPR-based detection methods have the potential to fulfill the urgent need for cheap, portable sensors capable of rapidly and sensitively detecting agents that pose a biological threat.[8–10] Only a limited number of studies exist utilizing SPR for the screening of pathogens[9,11–17] and explosives[18] compared to more sensitive surface bioaffinity measurements using fluorescence[19–21] and Raman[22,23] measurements. However, SPR is one of the very few techniques that provides non-invasive, multiplexed, real-time kinetic measurements while avoiding the need for on-site processing (*e.g.* labeling and enrichment) of the target sample prior to analysis.

Various novel enhancement methodologies have been created to improve both the sensitivity and selectivity of SPR biosensors. These include the design of various surface enzymatic amplification strategies[2,24–26] and also combining surface enzyme reactions with biofunctionalized nanoparticles.[27,28] Recently, we have developed a new technique, nanoparticle-enhanced diffraction gratings (NEDG), where the optical properties of planar surface plasmons generated on gold gratings are coupled with the optical properties of adsorbed gold nanoparticles to create ultrasensitive biosensors.[29] In this paper, we describe our efforts to combine the concepts of NEDG and surface enzymatic amplification for the sensitive detection of microRNA (miRNA) species. miRNA detection is particularly challenging due to its short sequence length (19–23 nucleotides), which inhibits the use of sandwich assays often utilized in conventional DNA analysis. Instead, an alternative strategy involving a surface poly(A) polymerase reaction followed by nanoparticle adsorption is employed. Fluorescence imaging measurements are also used to support and characterize the surface reactions. We show for the first time that the coupling of NEDG with surface enzymatic amplification leads to a promising new class of ultrasensitive bioaffinity sensors that can potentially be used in a large variety of biotechnology and biosecurity applications.

2. Experimental

Materials

11-Mercaptoundecylamine (MUAM; Dojindo), sulfosuccinimidyl 4-(*N*-maleimidomethyl)-cyclohexane-1-carboxylate (SSMCC; Pierce), *N*-hydroxysuccinimidyl ester of methoxy-poly(ethylene glycol) propionic acid MW 2000 (PEG-NHS; Nektar), dithiothreitol (DTT; Aldrich), polydimethylsiloxane

[a]*Department of Chemistry, Kyungpook National University, Daegu 702-701, Korea. E-mail: hyejinlee@knu.ac.kr*
[b]*Department of Pure and Applied Chemistry, University of Strathclyde, Glasgow, UK G1 1XL*
[c]*Department of Chemistry, University of California-Irvine, Irvine, CA 92697, USA*

† This paper is part of an *Analyst* themed issue on Detection for Security, with guest editors Andrew Bell and Pankaj Vadgama.

‡ The HTML version of this article has been enhanced with colour images.

(PDMS) curing agent and prepolymer (Sylgard 184, Dow Corning), yeast poly(A) polymerase (USB) and proteinase K (USB) were used as received. All thiol-modified locked nucleic acid (LNA) and DNA probes (Integrated DNA Technologies) were purified using binary reversed-phase HPLC and adjusted to a final concentration of 1 mM prior to use. The LNA probe sequences used for microarray fabrication were miR-122b-LNA = 5′-CCA TTG TCA CAC TCC A(C)$_{15}$(CH$_2$)$_3$-S-S-3′ and miR-16-LNA = 5′-TAT TTA CGT GCT GCT A(C)$_{15}$(CH$_2$)$_3$-S-S-3′ where all LNA bases are underlined. Both LNA probes were designed to have similar duplex melting temperatures upon complementary binding to their respective targets (www.exiqon.com). The 5′-thiol-modified DNA sequence used for the coating of Au nanoparticles for miRNA detection is 5′-S-S-(CH$_2$)$_6$-(T)$_{30}$-3′. The DNA sequences used in Fig. 2–4 are: D_1 = 5′-S-S-(CH$_2$)$_6$-(T)$_{15}$GTG TTA GCC TCA AGT G-3′, D_2 = 5′-GTC TAT GCG TGA ACT G(CH$_2$)$_6$-(T)$_{15}$-S-S-3′ and D_T = 5′-CAG TTC ACG CAT AGA CCA CTT GAG GCT AAC AC-3′. All synthetic miRNA sequences (Dharmacon RNA Technologies) were used as received. The miRNA sequences were: miR-122b = 5′-UGG AGU GUG ACA AUG GUG UUU GA-3′ and miR-16 = 5′-UAG CAG CAC GUA AAU AUU GGC G-3′. All rinsing steps were performed with either absolute ethanol or Millipore deionized water and all experiments were performed at room temperature.

Fabrication of gold grating chips

Gold grating chips were prepared using standard photolithography and lift-off techniques that are described elsewhere.[30] Fig. 1 outlines the procedure to create 5 (±1) μm gold lines with 10 (±2) μm spacing on SF-10 glass slides. The slides (18 × 18 mm, Schott Glass) were first soaked in piranha solution (3 : 1 mixture of 6 M sulfuric acid and 30% hydrogen peroxide) for 30 min followed by thorough rinsing with Millipore water and drying in an oven at 120 °C to remove any excess water. A positive photoresist (Microposit S1808™, Rohm and Haas Electronic Materials) was spin coated onto the slides (500 rpm for 10 s, 2500 rpm for 40 s), which were then baked at 90 °C for 30 min and cooled down to room temperature (Fig. 1, steps 1 and 2). Next, the slides were exposed for 10 s at 365 nm using a Karl Suss MJB3 aligner and a chrome mask featuring 5 μm Cr lines with 10 μm spacing (step 3). The patterned slides were immediately immersed in Microposit MF™-319 developer solution (Rohm and Haas Electronic Materials) for 20 s followed by rinsing with Millipore water, and drying in a gentle stream of nitrogen (step 4). This created a set of 10 (±2) μm lines of developed photoresist with 5 (±1) μm spacing on bare glass substrates. A thin layer of chromium (1 nm), followed by a layer of gold (45 nm) was deposited onto the slides using a Denton DV-502A metal evaporator (step 5). The slides were then kept in acetone for three days before sonication for 1 min in a 1 : 1 mixture of acetone and methanol followed by 1 min in Millipore water (step 6). Finally, the slides were rinsed thoroughly with Millipore water, and dried in a gentle stream of nitrogen. This results in the creation of arrays of gold lines whose measured width is about 6 μm [an optical microscope image of the grating is shown in Fig. 2(b)].

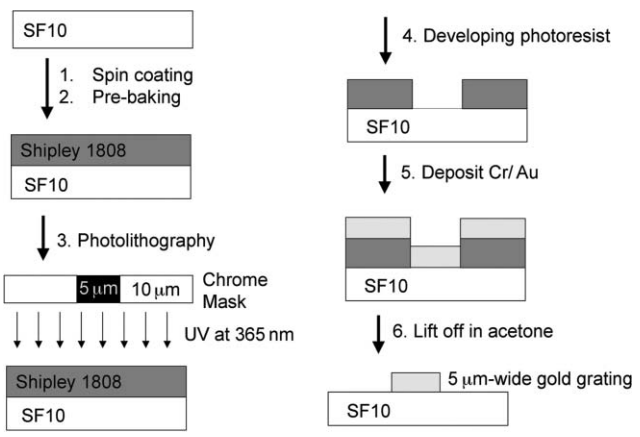

Fig. 1 An outline of the lift-off photolithography method used for the fabrication of gold line gratings on SF10 glass substrates. See the Experimental section for details on each of the six main fabrication steps involved to create gold grating lines 5 (±1) μm in width and 10 (±2) μm spacing on an SF10 glass substrate.

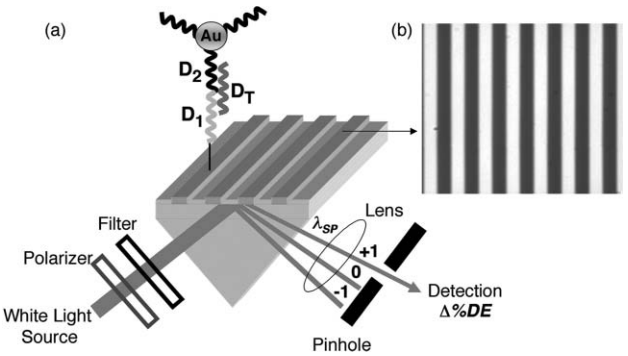

Fig. 2 (a) Schematic depicting the NEDG experimental setup for the detection of DNA. Collimated white light is passed through a polarizer and narrow bandpass filter (630 ± 10 nm) onto a prism/grating chip/flow cell assembly at a fixed incidence angle. Next, the +1 diffraction beam is collected through a lens and detected with either an optical fiber-coupled spectrometer or an avalanche photodiode (APD). Alternatively, the +1, 0, −1 orders are all imaged simultaneously on a CCD camera. (b) A partial optical microscope image of the diffraction grating which features 6 μm-wide and 45 nm-thick gold lines that extend along the entire length of the SF10 glass substrate with a grating period of 15 μm.

DNA and LNA surface immobilization on gold grating

Thiol-modified DNA or LNA was covalently immobilized onto the surface of the gold grating lines using a previously described cross-linkng chemistry.[31] Briefly, the gold diffraction gratings were first immersed in a 1 mM ethanolic MUAM solution for a minimum of 4 h to form a well-packed self-assembled monolayer. Next, the grating surface was reacted with a 1 mM solution of the heterobifunctional cross-linker SSMCC for 30 min. The SSMCC-modified grating surface was then allowed to react overnight with either 5′-thiol-modified DNA (D_1) or 3′-thiol-modified LNA (miR-122b-LNA). Finally, the DNA- or LNA-functionalized gold grating chip was rinsed in Millipore water and dried under a nitrogen stream prior to use.

Preparation of oligonucleotide-modified Au nanoparticles

A standard citrate reduction method[32] was used to synthesize Au nanoparticle solutions with a λ_{max} of 518 nm and an average particle diameter of apporximately 13 nm. DNA-modified Au nanoparticles were then prepared as follows:[27,28] 50 μL of either 100 μM 3′-thiol-modified DNA (D_2) or 5′-thiol-modified T_{30} oligonucleotide was added to 950 μL of Au nanoparticle stock solution and kept at 37 °C overnight. 350 μL of Millipore water and 150 μL of 1 M NaCl/100 mM phosphate (pH 7.4) were subsequently added to the solution and aged a further day at 37 °C. The excess DNA was then removed by centrifuging the nanoparticle solution at 13 000 rpm for 40 min, removing the supernatant and resuspending the Au pellet in 0.1 M NaCl/10 mM phosphate buffer (pH 7.4). This washing step was repeated three times before a final resuspension in 0.3 M NaCl/10 mM phosphate buffer (pH 7.4). The nanoparticle concentration was estimated to be 10 nM using UV-vis spectroscopy and an extinction coefficient of 2×10^8 M^{-1} cm^{-1}.

Surface enzyme reaction and hybridization reaction conditions

A three-step process was used for the detection of miRNAs:

(i) miRNA hybridization adsorption to LNA-modified surfaces. Selected concentrations of miRNA in 0.3 M NaCl/10 mM phosphate buffer (pH 7.4) were continuously flowed across the LNA microarray at a flow rate of 1 mL min^{-1} for 1 h. The hybridization reaction time necessary strongly depends upon the concentration of miRNA.

(ii) Surface polyadenylation reaction. After miRNA hybridization adsorption, LNA-immobilized surface was exposed to a mixture of yeast poly(A) polymerase (2.4 units μL^{-1}), 5 mM ATP in a reaction buffer of 20 mM Tris-HCl, 60 mM KCl, 4 mM $MnCl_2$, 0.5 mM DTT (pH 7.1) for 1 h. After the reaction, the surface was washed with a 100 nM proteinase K solution [50 mM Tris-HCl, 100 mM KCl, 5 mM $CaCl_2$ (pH 7.4)] for 30 min to remove any non-specifically adsorbed enzymes.

(iii) Signal amplification. A freshly prepared T_{30}-coated Au nanoparticle solution was exposed to the poly(A) tailed array surface for 10 min. For fluorescence measurements, a solution of 100 nM Cy5-labeled T_{24} was hybridized onto the surface-immobilized polyadenylated miRNA. All the surface hybridization adsorption experiments were performed in 0.3 M NaCl/10 mM phosphate buffer (pH 7.4). All buffers and deionized water used in the miRNA experiment were autoclaved prior to use.

Fluorescence measurements using microfluidic channels

A parallel set of PDMS microchannels was used to create a three-line pattern of LNA probes on a gold substrate.[33] Briefly, a set of parallel PDMS microchannels was physically attached to a MUAM-modified gold surface (commercial gold slides with 5 nm of Cr and 100 nm of Au from Evaporated Metal Films). The dimension of each channel is 75 μm wide, 1.2 cm long and 35 μm deep. A 1 mM solution of cross-linker SSMCC was flowed through each microchannel using a simple differential pumping system and allowed to react for 30 min. Solutions of 3′-thiol-modified miR-122b-LNA and miR-16-LNA (1 mM) were then injected into separate channels and reacted overnight to create LNA line arrays; miR-122b-LNA was introduced into both outer channels, while miR-16-LNA was injected into the middle channel. The first set of PDMS microchannels was then removed and replaced with a second set of PDMS microchannels arranged perpendicular to the surface line pattern. The channel intersections create discrete fluorescence imaging detection regions (75 × 75 μm). A 1 mM solution of PEG-NHS was introduced through each channel to surround the detection regions with a PEG background that is resistant to non-specific adsorption. Next, a solution containing 50 pM miR-122b was flowed through each channel for 1 h followed sequentially by the poly(A) polymerase reaction and hybridization of Cy5-labeled T_{24} DNA.

3. Results and discussion

3.1. Characterization of NEDG biosensor

In an attempt to further improve the sensitivity of surface plasmon biosensors, we recently developed a novel approach that combines the concepts of optical diffraction and nanoparticle-enhanced detection.[29] An outline of the nanoparticle-enhanced diffraction grating method (termed NEDG) is shown in Fig. 2. A grating consisting of 6 μm-wide, 45 nm-thick parallel gold lines with a grating periodicity of 15 μm is optically coupled to a prism (Kretchmann configuration). The gold grating is illuminated through the prism at a chosen angle of incidence using a p-polarized collimated white light source that can also be filtered to transmit a selected wavelength. The grating is aligned perpendicular to the plane of incidence of the light source, generating a linear series of diffracted spots in the incidence plane. Planar surface plasmons are excited across the grating lines whose 6 μm width is on the order of plasmon propagation length at the vis-NIR wavelengths. Upon the adsorption of biofunctionalized nanoparticles onto the grating, shifts in the reflected intensity at the first order (+1) diffraction spot are measured to calculate the relative change in the first order diffraction efficiency ($\Delta\%DE$). The analysis of individual diffraction spots is achieved using either a fiber-coupled spectrometer to obtain a diffraction spectrum, or by first filtering the white light source and using an avalanche photodiode (APD). A CCD camera can also be used to analyze multiple diffraction spots simultaneously.

The NEDG biosensor was first characterized using a simple nanoparticle sandwich adsorption assay to detect DNA. Prior to performing this measurement the dependence of the surface plasmon excitation on both the wavelength and incident angle of the light source must be considered. The incident angle is selected experimentally by first replacing the diffraction grating with a continuous gold film. Next, the prism/gold chip assembly is rotated with respect to the light source until a strong minimum is observed in the reflectance spectrum around 633 nm [see Fig. 3(a)]. This wavelength region was targeted for the excitation of surface plasmons on the grating because the local plasmon resonance of the individual gold nanoparticles ($\lambda_{max} \approx 520$ nm) will shift considerably into the red upon adsorption onto the grating surface. The corresponding input angle is denoted as the plasmon angle (θ_{SP}), which is equal to 57.2 ° at 633 nm. Following this step, the planar gold film is replaced by a grating surface and

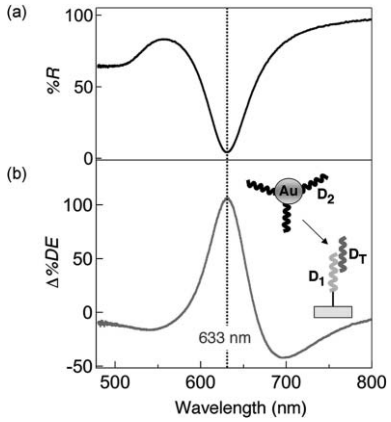

Fig. 3 (a) Reflectance spectrum acquired using a fiber-coupled spectrometer for a continuous planar 45 nm gold film in contact with water. An incident angle of 57.2 ° is selected to excite surface plasmons at a wavelength region around 630 nm. (b) Spectral measurement of the relative change in diffraction efficiency ($\Delta\%DE$) at the +1 diffraction spot due to the adsorption of DNA (D_2)-functionalized nanoparticles onto D_1-immobilized gold grating surfaces that had been previously exposed to a 100 nM target DNA (D_T) solution. The incident angle was adjusted to 56.6 ° to obtain a maximum increase in diffraction efficiency at the targeted plasmon wavelength.

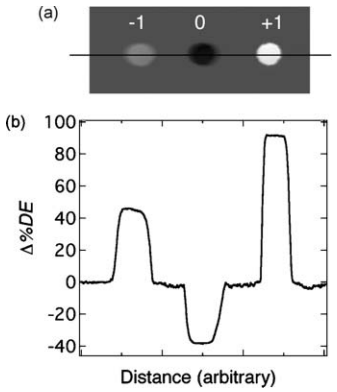

Fig. 4 (a) NEDG difference image and (b) corresponding quantitative line profile for the sandwich assay detection of a 100 nM solution of D_T. The relative diffraction efficiency ($\Delta\%DE$) was calculated using the equation [$\Delta\%DE = 100\ (I_{NP} - I_0)/I_0$], where I_0 and I_{NP} are the images acquired before and after the nanoparticle adsorption step respectively. The experimental conditions were the same as those described in Fig. 3(b). A maximum signal increase of 92% was observed at the first order diffraction spot.

the incident angle (θ_i) adjusted according to the equation $\theta_i = \theta_{SP} - \Delta/2$ where Δ is the separation angle between the zero- and first-order beams and was measured at 1.2°. This adjustment is necessary to obtain a maximum change in diffraction efficiency at the targeted plasmon wavelength.

DNA detection is achieved using a grating surface upon which a monolayer of single-stranded DNA (ssDNA) molecules (D_1) is immobilized. D_1 is complementary to half of the sequence of the target ssDNA molecule (D_T). The grating is then exposed to a solution of D_T resulting in hybridization adsorption of the target to form D_1–D_T duplexes. Next, a solution of gold nanoparticles functionalized with an ssDNA sequence (D_2) that is complementary to the other half of D_T is flowed across the grating and changes in the NEDG signal are recorded. Fig. 3(b) shows a spectrum of the relative change in the first order diffraction efficiency ($\Delta\%DE$) measured at the +1 diffraction spot due to the adsorption of D_2-modified gold nanoparticles onto the surface D_1–D_T duplexes. To ensure full surface coverage, a 100 nM solution of D_T was employed with $\Delta\%DE$ calculated by comparing +1 spot intensities before and after nanoparticle hybridization adsorption. The remarkable 100% increase in diffraction efficiency measured at the targeted plasmon frequency of 633 nm indicates saturation of the NEDG signal response. Also shown in Fig. 4(a) is a NEDG difference image of the +1, 0 and −1 diffraction spots obtained by comparing CCD camera images acquired *via* a 633 nm filter before and after adsorption of the D_2–nanoparticle conjugate onto the surface D_1–D_T duplexes. The positive increase in signal observed at the −1 diffraction spot is about half that of the +1 signal while at the zero order spot a negative change in $\Delta\%DE$ is actually recorded [see Fig. 4(b)]. It is clear that the direction and magnitude of the response differ for each diffraction order, as reported previously for diffraction-based sensors.[34] In addition, the relative differences in magnitude between each diffraction order signal will vary with the incident angle at which the measurement is performed.

3.2 miRNA detection with enzymatically-amplified NEDG and fluorescence

miRNAs are a recently-discovered class of non-protein coding RNA molecules thought to play a controlling role in gene expression,[35,36] with aberrations in miRNA expression levels being linked to a variety of diseases, including cancer.[37,38] However, the short length of miRNA (19–23 nucleotides) introduces additional challenges that prevents the use of conventional approaches (such as the sandwich assay described in the previous section) typically used for DNA microarray analyses. Instead, an amplification approach that combines a surface poly(A) polymerase reaction and DNA-modified nanoparticles is used for the sensitive NEDG sensing of miRNA.

An outline of the scheme for the NEDG detection and identification of microRNAs is shown in Fig. 5(a). The first step is the sequence-specific hybridization adsorption of the miRNA target onto a single-stranded LNA probe immobilized on the gold grating pattern. LNAs are nucleic acid analogues containing one or more chemically-modified nucleotides with the RNA–LNA binding strength at least ten times greater than that associated with RNA–DNA heteroduplex formation.[39] The presence of surface-bound miRNA is detected with NEDG following the growth of a poly(A) tail *via* a poly(A) polymerase surface reaction and then hybridization of T_{30} DNA-coated gold nanoparticles. Fig. 5(b) and 5(c) show the $\Delta\%DE$ signal measured at the −1, 0 and +1 diffraction spots for the detection of the miRNA sequence miR-122b at a concentration of 50 pM. As expected from the previous section, the largest change in the NEDG response (about 5.7%) was observed at the +1 spot with a smaller increase at the −1 spot and a decrease in signal at the zero order. When the experiment was repeated using a sequence (miR-16) that is not complementary to the LNA probe, no measurable signal was observed.

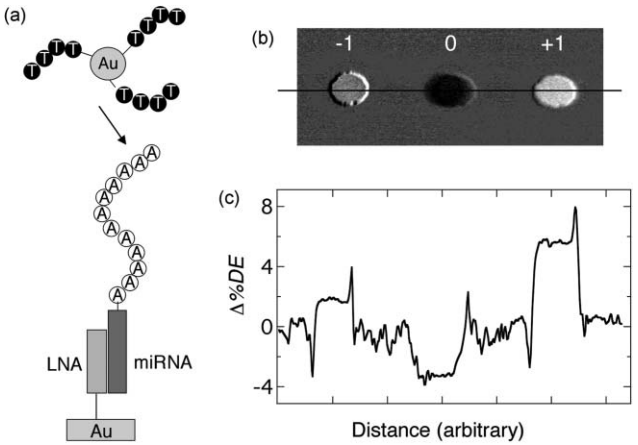

Fig. 5 Detection of a 50 pM solution of miRNA using a combination of NEDG and polyadenylation-nanoparticle surface amplification. (a) Schematic of the miRNA detection scheme. Briefly, the miRNA target (miR-122b) was first specifically hybridized onto an LNA probe (miR-122b-LNA) previously immobilized on a gold grating surface. Poly(A) polymerase was then reacted with the surface attached miRNA–LNA heteroduplex for 30 min resulting in the addition of a poly(A) tail to the miRNA strand. After washing, the grating surface was exposed to a solution of T_{30}-coated nanoparticles for 10 min. The NEDG difference image (b) and the corresponding line profile (c) were obtained by subtracting images acquired before and after the adsorption of T_{30}-modified nanoparticles onto the poly(A) tails of the miRNA strand. The equation described in the Fig. 4 caption was used to obtain $\Delta\%DE$ with the largest change at the first order spot measured at 5.7%.

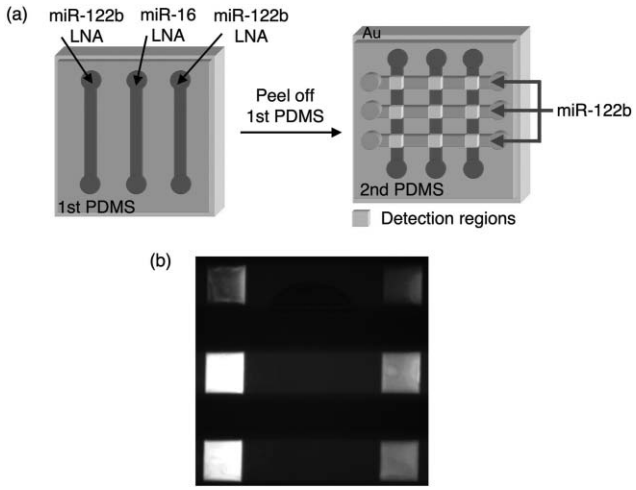

Fig. 6 Fluorescence imaging detection of 50 pM miR-122b using surface polyadenylation followed by hybridization of Cy5-labeled T_{24} DNA. (a) Schematic outlining a two-step PDMS microfluidic array fabrication and detection process; a set of parallel PDMS microchannels (75 μm wide, 35 μm wide and 1.2 cm long) was first physically attached to the MUAM-modified gold surface. SSMCC was flowed through each channel and miR-122b-LNA was then injected into both outer channels, while miR-16-LNA was injected into the middle channel. After LNA probe immobilization, the microchannels were removed and replaced with a second set of channels orientated perpendicular to the surface line pattern and used to sequentially deliver small volumes of (2 μL) of PEG-NHS (1 mM), miR-122b (50 pM), poly(A) polymerase (2.4 units μL^{-1}) and Cy5-labeled T_{24} DNA (100 nM) solutions to each channel. (b) Fluorescence image showing Cy5-labeled DNA hybridization onto the poly(A) tails formed on miR-122b previously hybridized to miR-122b-LNA probes. Fluorescence was observed only at regions where the miR-122b-LNA probe lines and miR-122b delivery channels intersect.

In a final experiment, fluorescence imaging measurements were performed to verify the specificity and sensitivity of the miRNA measurements using NEDG. Microfluidics were used to create a 2-D hybridization line array on a planar gold surface.[33] As outlined in Fig. 6(a), an initial set of parallel microfluidic channels was first applied to direct the surface immobilization of both miR-122b-LNA and miR-16-LNA probe molecules. Following replacement of the first set of channels with a second set placed in a perpendicular direction, a solution of 50 pM miR-122b target was then injected into each channel allowing 1 h for hybridization. Next, the poly(A) polymerase reaction solution and a 100 nM solution of Cy5-labeled T_{24} DNA were flowed sequentially through each channel. A significant fluorescence signal [see Fig. 6(b)] was obtained only where the miR-122b-LNA probe lines and the miR-122b target delivery channels intersect, with no detectable signal observed for the non-complementary miR-16-LNA probe sequence or on the PEG background.

The sensitivity of these fluorescence measurements is comparable with the NEDG measurements shown previously in Fig. 5 with good signal-to-noise observed in both cases at a target concentration of 50 pM. However, for the NEDG measurements a simple, non-cooled CCD camera was used in comparison to the high-end fluorescence microscope utilized to acquire the imaging data in Fig. 6. Consequently, we expect that the sensitivity of the NEDG measurements will be dramatically improved by replacing the CCD camera with an avalanche photodiode and lock-in techniques to allow much smaller changes in $\Delta\%DE$ to be easily measured at the first order diffraction spot. Using this approach for the DNA sandwich assay described in Fig. 3, a detection limit of around 10 fM was established,[29] which is over 100 times more sensitive than comparable measurements using either nanoparticle-enhanced SPRI[40] or fluorescence microarrays.[41] We also anticipate that further optimization of the surface enzyme reaction on the grating as well as exploring NEDG measurements at different resonance wavelengths in the vis-NIR region utilizing nanoparticles with different sizes and shapes will also lead to further improvements in performance.

4. Conclusions

In this paper, we have presented a novel methodology for surface bioaffinity sensing that uses a unique combination of a surface polymerase reaction in conjunction with nanoparticle adsorption onto an optical diffraction grating that supports the excitation of planar surface plasmons. Nanoparticle-enhanced diffraction gratings (NEDG) are a promising new class of biosensors whose utility can be further extended by incorporating surface enzymatic amplification strategies, as demonstrated here for miRNA detection.

The NEDG platform can easily be reduced in size, which will allow incorporation into microfluidic devices and also promote multiplexed detection. In addition, the ability to tune the plasmon excitation wavelength in the gratings will enable further optimization using different nanoparticles sizes and materials. We fully expect that NEDG will develop into an

important class of surface bioaffinity sensors for biotechnology- and biosecurity-related research and applications.

Acknowledgements

The authors acknowledge funding support from the National Institutes of Health (2RO1 GM059622-08) and the National Science Foundation (CHE-0551935).

References

1 Y. Li, H. J. Lee and R. M. Corn, *Anal. Chem.*, 2007, **79**, 1082–1088.
2 H. J. Lee, A. W. Wark and R. M. Corn, *Langmuir*, 2006, **22**, 5241–5250.
3 K. S. Phillips, J.-H. Han, M. Martinez, Z. Wang, D. Carter and Q. Cheng, *Anal. Chem.*, 2006, **78**, 596–603.
4 V. Kanda, P. Kitov, D. R. Bundle and M. T. McDermott, *Anal. Chem.*, 2005, **77**, 7497–7504.
5 L. K. Wolf, D. E. Fullenkamp and R. M. Georgiadis, *J. Am. Chem. Soc.*, 2005, **127**, 17453–17459.
6 M. Kyo, K. Usui-Aoki and H. Koga, *Anal. Chem.*, 2005, **77**, 7115–7121.
7 J. S. Shumaker-Parry and C. T. Campbell, *Anal. Chem.*, 2004, **76**, 907–917.
8 B. Pejcic, R. De Marco and G. Parkinson, *Analyst*, 2006, **131**, 1079–1090.
9 Y. Amano and Q. Cheng, *Anal. Bioanal. Chem.*, 2005, **381**, 156–164.
10 D. V. Lim, J. M. Simpson, E. A. Kearns and M. F. Kramer, *Clin. Microbiol. Rev.*, 2005, **18**, 583–607.
11 V. Nanduri, A. K. Bhunia, S.-I. Tu, G. C. Paoli and J. D. Brewster, *Biosens. Bioelectron.*, 2007, **23**, 248–252.
12 A. Subramanian, J. Irudayaraj and T. Ryan, *Biosens. Bioelectron.*, 2006, **21**, 998–1006.
13 S. C. B. Gopinath, T. S. Misono, K. Kawasaki, T. Takafumi Mizuno, M. Imai, T. Odagiri and P. K. R. Kumar, *J. Gen. Virol.*, 2006, **87**, 479–487.
14 A. J. Haes, L. Chang, W. L. Klein and R. P. Van Duyne, *J. Am. Chem. Soc.*, 2005, **127**, 2264–2271.
15 S. Chen, L. Chen, J. Tan, J. Chen, L. Du, T. Sun, J. Shen, K. Chen, H. Jiang and X. Shen, *J. Biol. Chem.*, 2005, **280**, 164–173.
16 T. S. Misono and P. K. R. Kumar, *Anal. Biochem.*, 2005, **342**, 312–317.
17 P. Gomes, E. Giralt and D. Andreu, *Vaccine*, 2000, **18**, 362–370.
18 D. R. Shankaran, T. Kawaguchi, S. J. Kim, K. Matsumoto, K. Toko and N. Miura, *Anal. Bioanal. Chem.*, 2006, **386**, 1313–1320.
19 L. Song, S. Ahn and D. R. Walt, *Anal. Chem.*, 2006, **78**, 1023–1033.
20 S. Sengupta, K. Onodera, A. Lai and U. Melcher, *J. Clin. Microbiol.*, 2003, **41**, 4542–4550.
21 N. Sergeev, M. Distler, S. Courtney, S. F. Al-Khaldi, D. Volokhov, V. Chizhikov and A. Rasooly, *Biosens. Bioelectron.*, 2004, **20**, 684–698.
22 S. Shanmukh, L. Jones, J. Driskell, Y. Zhao, R. Dluhy and R. A. Tripp, *Nano Lett.*, 2006, **6**, 2630–2636.
23 J. D. Driskell, K. M. Kwarta, R. J. Lipert, M. D. Porter, J. D. Neill and J. F. Ridpath, *Anal. Chem.*, 2005, **77**, 6147–6154.
24 Y. Li, H. J. Lee and R. M. Corn, *Nucleic Acids Res.*, 2006, **34**, 6416–6424.
25 H. J. Lee, Y. Li, A. W. Wark and R. M. Corn, *Anal. Chem.*, 2005, **77**, 5096–5100.
26 T. T. Goodrich, H. J. Lee and R. M. Corn, *J. Am. Chem. Soc.*, 2004, **126**, 4086–4087.
27 S. Fang, H. J. Lee, A. W. Wark and R. M. Corn, *J. Am. Chem. Soc.*, 2006, **128**, 14044–14046.
28 Y. Li, A. W. Wark, H. J. Lee and R. M. Corn, *Anal. Chem.*, 2006, **78**, 3158–3164.
29 A. W. Wark, H. J. Lee, A. J. Qavi and R. M. Corn, *Anal. Chem.*, 2007, **79**, 6667–6701.
30 E. J. Menke, M. A. Thomson, C. Xiang, L. C. Yang and R. M. Penner, *Nat. Mater.*, 2006, **5**, 914–919.
31 J. M. Brockman, A. G. Frutos and R. M. Corn, *J. Am. Chem. Soc.*, 1999, **121**, 8044–8051.
32 K. C. Grabar, R. G. Freeman, M. B. Hommer and M. J. Natan, *Anal. Chem.*, 1995, **67**, 735–743.
33 H. J. Lee, T. T. Goodrich and R. M. Corn, *Anal. Chem.*, 2001, **73**, 5525–5531.
34 R. C. Bailey, J.-M. Nam, C. A. Mirkin and J. T. Hupp, *J. Am. Chem. Soc.*, 2003, **125**, 13541–13547.
35 L. He and G. J. Hannon, *Nat. Rev. Genet.*, 2004, **5**, 522–531.
36 D. Bartel, *Cell*, 2004, **116**, 281–297.
37 G. A. Calin and C. M. Croce, *Nat. Rev. Cancer*, 2006, **6**, 857–866.
38 A. Esquela-Kerscher and F. J. Slack, *Nat. Rev. Cancer*, 2006, **6**, 259–269.
39 M. Castoldi, S. Schmidt, V. Benes, M. Noerholm, A. E. Kulozik, M. W. Hentze and M. U. Muckenthaler, *RNA*, 2006, **12**, 913–920.
40 L. He, M. D. Musick, S. R. Nicewarner, F. G. Salinas, S. J. Benkovic, M. J. Natan and C. D. Keating, *J. Am. Chem. Soc.*, 2000, **122**, 9071–9077.
41 T. Livache, E. Maillart, N. Lassalle, P. Mailley, B. Corso, P. Guedon, A. Roget and Y. Levy, *J. Pharm. Biomed. Anal.*, 2003, **32**, 687–696.